Journal of Materials Chemistry C

PAPER

View Article Online
View Journal | View Issue

Cite this: J. Mater. Chem. C, 2015, 3, 5316

One-pot synthesis of hydrophobic and enhanced red-emitting $CaCO_3:Eu^{3+}$ phosphors

Yidi Sun,[a] Haifeng Zou,[a] Bowen Zhang,[a] Xiuqing Zhou,[a] Qisheng Huo[b] and Ye Sheng*[a]

Received 10th March 2015,
Accepted 23rd April 2015

DOI: 10.1039/c5tc00681c

www.rsc.org/MaterialsC

Enhanced red-emitting $CaCO_3:Eu^{3+}$ phosphors were *in situ* prepared using the carbonization method in the presence of sodium oleate. It has been proved that the introduction of sodium oleate can endow the products with a hydrophobic surface, which makes the products exhibit good compatibility with plastics or other polymers. Remarkably, the addition of sodium oleate can also enhance the red emission intensity of $CaCO_3:Eu^{3+}$ phosphors greatly compared to that of the common $CaCO_3:Eu^{3+}$ phosphors. The enhancement is attributed to two functions of sodium oleate. One function is that sodium oleate can avoid OH ligands and/or crystal water molecules attached on the surface of $CaCO_3$ particles; the other function is that Na^+ ions can supply effective charge compensation.

1. Introduction

Inorganic phosphors doped with rare earth ions have attracted extensive attention owing to their remarkable luminescence properties and applications.[1–3] As an efficient red luminescent activator, trivalent europium (Eu^{3+}) was widely doped in the hosts of titanate,[4,5] silicate,[6,7] aluminosilicate,[8] fluoride,[9–11] oxysulfide,[12,13] and metal oxide.[14] The synthesis methods include the high-temperature solid-state reaction method[15] and wet chemistry methods such as co-precipitation,[16,17] hydrothermal synthesis,[18–20] colloidal chemistry[21] *etc*. However, the phosphors prepared by a solid-state reaction method have a big enough crystallite size, irregular morphology, and high hardness, which are not good for luminescence in application. Therefore, the phosphors must be ground, which produces defects that can act as non-radiative recombination sites degrading the luminescence efficiency.[22] On the other hand, most phosphors prepared by wet chemistry methods crystallize and exhibit luminescence only after being sintered at high temperature, because OH ligands and/or crystal water molecules attached on the surface or in the host lattice of the particles, which may quench luminescence, are unavoidable and the precursors from wet chemical methods are generally amorphous.[23,24] Consequently, it is necessary to further sinter these precursors at higher temperature in most cases. Herein, there has been ongoing interest in the preparation and luminescent behaviors of the red phosphor of the $CaCO_3$ matrix because it can be prepared at low temperature with good crystallinity and regular morphology and can exhibit strong red emission without any further treatment.[25–31]

$CaCO_3$ is one of the important fillers used in the industries of plastics, rubbers, paint, and so on. Such industrial applications require well-refined and well-dispersed $CaCO_3$ particles.[32,33] However, the nano-sized $CaCO_3$ particles tend to aggregate together. Furthermore, like most inorganic fillers, they have polar, hydrophilic, and high free energy surfaces and are incompatible with some nonpolar, hydrophobic, and low free energy polymer matrices. Surface modification of $CaCO_3$ with hydrophobic species would lead to a great expansion in these applications, since mineral particles are hardly dispersed in a polymer matrix.

It is well known that the synthesis of $CaCO_3$ is usually followed by two basic synthesis routes: (1) the solution route, through a double decomposition reaction, wherein calcium salts (*e.g.* $CaCl_2$) and soluble carbonates (*e.g.* Na_2CO_3) are combined with an equal molar ratio; (2) the carbonation method, in which CO_2 gas is bubbled through an aqueous slurry of $Ca(OH)_2$. The latter route is preferred in terms of environmental protection and the effective use of mineral resources[34] and it is an industrially useful method. All the Re-doped $CaCO_3$ phosphors reported were prepared by the solution route, and we first reported a study on the $CaCO_3:Eu^{3+}$ phosphors prepared by the carbonation method.[29]

On the basis of our previous work, hydrophobic and enhanced red-emitting $CaCO_3:Eu^{3+}$ phosphors were *in situ* prepared *via* the carbonization method in the presence of sodium oleate. The obtained products are in a powder form. Furthermore, they not only have hydrophobic surfaces, which make them exhibit good compatibility with plastics or other polymers, but also have enhanced red emission of Eu^{3+} under ultraviolet excitation. The enhancement of photoluminescence intensities of the

[a] College of Chemistry, Jilin University, Changchun 130012, P. R. China. E-mail: shengye@jlu.edu.cn; Fax: +86-431-85155275; Tel: +86-431-85168428
[b] State Key Laboratory of Inorganic Synthesis and Preparative Chemistry, College of Chemistry, Jilin University, Changchun 130012, P. R. China

modified sample was attributed to the charge compensation of sodium ions and the reduction of OH ligands and/or crystal water molecules attached on the surface of $CaCO_3$ particles.

2. Experimental

2.1. Materials

Calcium oxide (CaO), sodium oleate and Eu_2O_3 (99.99%) were bought from Beijing Chemical Reagents Co. All chemicals were analytical grade reagents and were used directly without further purification. $Eu(NO_3)_3$ aqueous solution was obtained by dissolving Eu_2O_3 (99.99%) in a dilute HNO_3 solution under heating with constant agitation. Distilled water was used.

2.2. Preparation

2.2.1. *In situ* preparation of $CaCO_3$ doped with Eu^{3+}. $CaCO_3$ doped with Eu^{3+} nanoparticles was synthesized as reported previously.[29] Typically, a certain amount of calcium oxide (CaO) was digested in distilled water to form a calcium hydroxide ($Ca(OH)_2$) slurry, which was kept overnight. A certain amount of $Eu(NO_3)_3$ aqueous solution (the molar ratio of $CaCO_3$ and Eu^{3+} was 50 : 1) was added into the $Ca(OH)_2$ slurry and stirred for 0.5 h, and then the slurry was transferred into a bubble glass column with an inner diameter (i.d.) of 3 cm and a gas inlet tube with an i.d. of *ca.* 0.8 cm was placed just above the bottom of the column. A mixed gas of carbon dioxide (CO_2) and nitrogen (N_2) with a molar ratio of 1 : 2 was introduced into the slurry through the tube. Bubbling of the gas mixture was stopped as soon as the pH of the slurry decreased to 7. Finally the precipitates were centrifugally separated from their mother liquor and washed three times with distilled water. The final product was dried in an oven at 80 °C for 24 h.

2.2.2. *In situ* preparation of hydrophobic $CaCO_3$ doped with Eu^{3+}. Different amounts of sodium oleate were added when CaO was digested, and the procedure is the same as that described in Section 2.2.1.

2.3. Characterization

X-ray powder diffraction measurements were carried out on a Rigaku D/max-B II X-ray diffractometer with Cu Ka radiation. The field emission scanning electron microscopy (FESEM) images were observed using S-4800. Fourier transform infrared (FT-IR) spectra were recorded on a Perkin-Elmer 580B infrared spectrophotometer using the KBr pellet technique. Thermogravimetric analysis (TGA) was performed using a TGA/SDTA851e analyzer (Mettler Toledo) over a temperature range of 50–900 °C in an air atmosphere with a heating rate of 10 °C min^{-1}. The PL measurements were determined using a Jobin Yvon FluoroMax-4 luminescence spectrophotometer equipped with a 150 W xenon lamp as the excitation source.

The effect of surface modification is evaluated by the contact angle and the active ratio measurement. The floating test was used to measure the ratio of the floating product to the overall weight of the sample after mixing in water and stirring vigorously. The ratio is called an active ratio. The higher the active ratio and the contact angle, the better the modification effect is. The contact angle of the product was measured using a FTA200 (USA) contact angle analyzer. In practice, discs were prepared by compressing, under controlled conditions, 200 mg of $CaCO_3$ in a typical IR die. Reproducible wetting data were observed on discs prepared at 10 MPa pressure.

3. Results and discussion

It is well known that nanoparticles are prone to aggregate together. In our experiments, $CaCO_3$:Eu^{3+} nanoparticles prepared without addition of sodium oleate are some hard blocks and it is necessary to grind them into powders. In contrast, $CaCO_3$:Eu^{3+} samples prepared in the presence of sodium oleate are in the powder form. They are all characterized in detail and the results are discussed as follows.

3.1. Structural properties

Fig. 1 shows the XRD patterns of the $CaCO_3$:Eu^{3+} products prepared using the carbonization method with different amounts of sodium oleate. The XRD results show that the diffraction peaks of all the products can be exactly assigned to the standard diffraction data of calcite $CaCO_3$ (JCPDS No. 47-1743). No characteristic peaks of other impurities were detected, indicating that the products have high purity and the Eu^{3+} ions and sodium oleate have not changed the crystal structure of $CaCO_3$.

The SEM images of the $CaCO_3$:Eu^{3+} nanoparticles prepared with and without sodium oleate are shown in Fig. 2. It can be seen that they are all cube-like and their sizes are about 20 nm. Compared with $CaCO_3$:Eu^{3+} without the addition of sodium oleate, the sizes of the products with sodium oleate change little but the dispersion becomes better. It was shown that the addition of sodium oleate improved the dispersion of $CaCO_3$, which would endow good compatibility with plastics or other polymers.

FT-IR spectra of the obtained products are shown in Fig. 3. It is indicated that all samples exhibited characteristic absorption peaks at 710 cm^{-1}, 875 cm^{-1}, 1459 cm^{-1} and 3440 cm^{-1}. The broad absorption peak at 3440 cm^{-1} is due to the symmetric

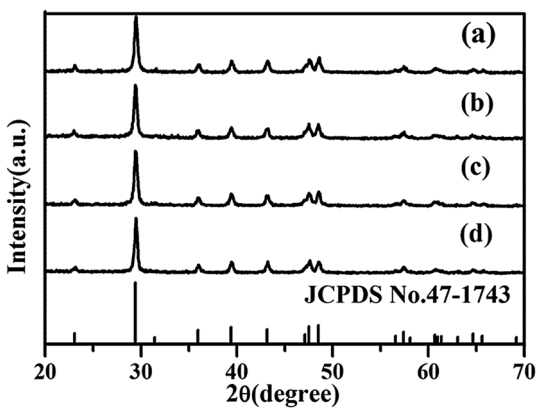

Fig. 1 XRD patterns of $CaCO_3$:Eu^{3+} samples prepared with different amounts of sodium oleate. (a) 0.0% W_{CaCO_3}; (b) 2.0% W_{CaCO_3}; (c) 5.0% W_{CaCO_3}; and (d) 10.0% W_{CaCO_3}.

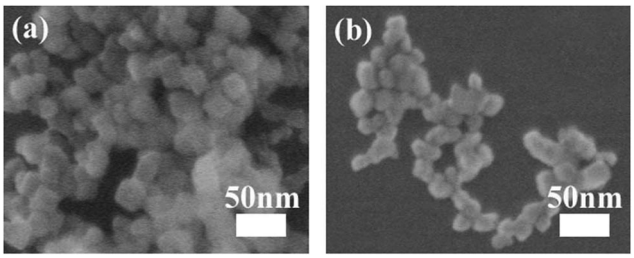

Fig. 2 SEM images of the $CaCO_3$:Eu^{3+} products prepared without (a) or with 5.0 wt% sodium oleate (b).

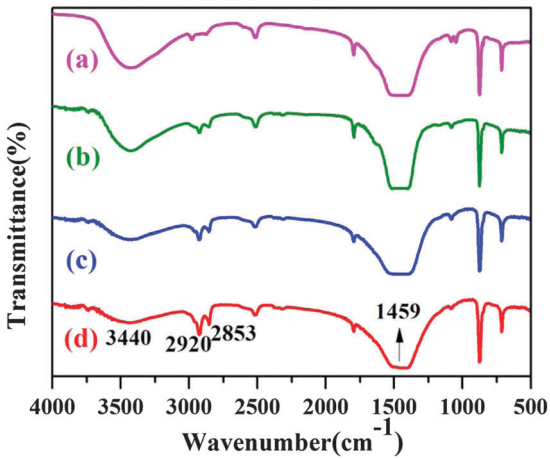

Fig. 3 FT-IR spectra of the $CaCO_3$:Eu^{3+} products prepared with different amounts of sodium oleate. (a) 0.0% W_{CaCO_3}; (b) 2.0% W_{CaCO_3}; (c) 5.0% W_{CaCO_3}; and (d) 10.0% W_{CaCO_3}.

and asymmetric stretching vibration generated by –OH.[35] It can be found that the intensity of this peak decreased with an increase of the amount of sodium oleate, indicating that the –OH ligands and/or crystal water molecules attached on the $CaCO_3$ particle surface or in the host lattice have been reduced with the addition of sodium oleate. The strong absorption peak near 1459 cm^{-1} is the characteristic absorption of $CaCO_3$, which is assigned to the asymmetric stretching vibration of C═O.[28] It is obvious that the absorption peak at 1459 cm^{-1} was broadened with an increase of the amount of sodium oleate, indicating the bonding between calcium ions and carboxylate of sodium oleate.[34] In addition, the intensity of the absorption peaks at around 2920 cm^{-1} and 2853 cm^{-1} in the modified products increased with an increase of the amount of sodium oleate, which is the characteristic of H–C–H asymmetric and symmetric stretching vibrations, respectively. This is attributed to the organic moieties of sodium oleate bonded onto the surface of calcium carbonate.[36]

Fig. 4 shows the TGA curves of unmodified and modified particles with sodium oleate. It has been proved that the hydrophobic property was attributed to the deposition of calcium oleate, produced in the reaction mixture, onto the surface of calcium carbonate particles and the decomposition peaks of calcium oleate are at around 280 °C and 475 °C.[37] Therefore, the TGA curves can be divided into three steps: the first step is

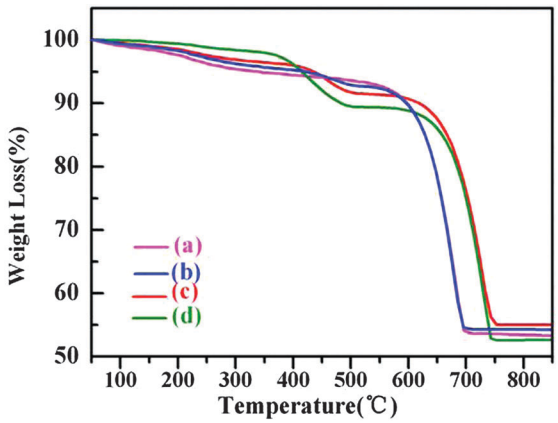

Fig. 4 The thermogravimetric curves of the $CaCO_3$:Eu^{3+} products prepared with different amounts of sodium oleate. (a) 0.0% W_{CaCO_3}; (b) 2.0% W_{CaCO_3}; (c) 5.0% W_{CaCO_3}; and (d) 10.0% W_{CaCO_3}.

before 300 °C, the weight loss of this step is due to the loss of the adsorption water and organic moieties on the surface of calcium carbonate particles. It can be inferred that the amount of water adsorbed on the surface of calcium carbonate particles reduced with an increase of the amount of sodium oleate. The second step is from 300 °C to 500 °C, the weight loss of this part is due to the decomposition of calcium oleate, and its value is nearly the same as the dosage of sodium oleate. It should also be noted that in the second stage the onset temperature of the samples with 10.0 wt% sodium oleate is lower than that of other two samples. It might be attributed to the following two reasons. One reason is the lower content of calcium oleate formed for the samples of 2.0 wt% and 5.0 wt% sodium oleate. From the TG and DTG traces of calcium oleate,[37] the onset decomposition temperature of the second step of calcium oleate is found to be 320 °C; it is not obvious for the lower content of calcium oleate. The other reason is that there exist excess organic moieties for the samples with 10.0 wt% sodium oleate. The third weight loss occurs after 550 °C, which indicates that $CaCO_3$ begins to decompose at that temperature. From Fig. 4, it can be concluded that the addition of sodium oleate reduced the amount of water adsorbed on the surface of calcium carbonate and did not lower the thermal stability of $CaCO_3$.

3.2. Hydrophobic properties

The active ratio of products is shown in Fig. 5. It can be seen that the active ratio increased with an increase in the amount of sodium oleate and reached 91.0% when the dosage of sodium oleate was 5.0%.

The contact angle was frequently used to measure the extent of hydrophobicity of solid surfaces. The contact angle of the products with different amounts of sodium oleate is shown in Fig. 6. From Fig. 6a, it can be seen that the water droplets dropped on thin pellets of $CaCO_3$ powders did not change the shape, but were imbibed in the pellets and the relative contact angle was only 26°. This phenomenon indicated that pure $CaCO_3$ was hydrophilic and was easily wetted by water. When 2.0 wt% sodium oleate was added, the hydrophobicity was increased, and the relative

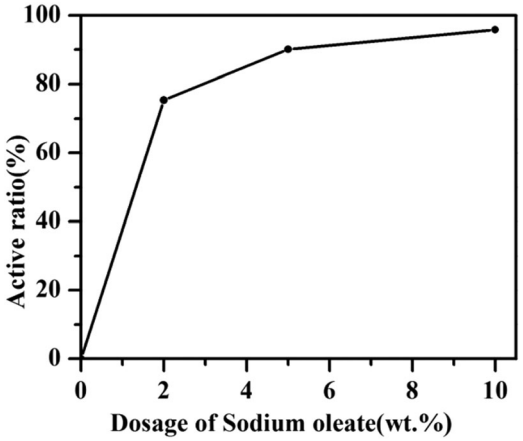

Fig. 5 The influence of the dosage of sodium oleate on the active ratio of the products.

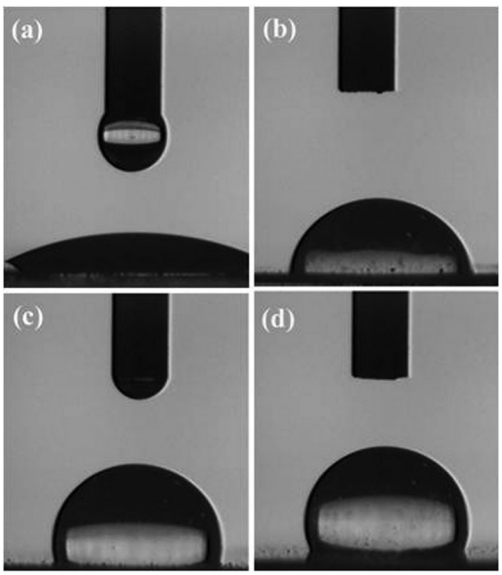

Fig. 6 The images of the contact angle of $CaCO_3$:Eu^{3+} with different amounts of sodium oleate: (a) 0.0% W_{CaCO_3}; (b) 2.0% W_{CaCO_3}; (c) 5.0% W_{CaCO_3}; and (d) 10.0% W_{CaCO_3}.

contact angle was increased to 78° (Fig. 6b). Upon increasing the amount of sodium oleate to 5.0 wt%, the relative contact angle reached 99.99° (Fig. 6c). This indicated that the hydrophobic surface formed when the weight ratio of SO/$CaCO_3$ was above 5.0%. Upon increasing the amount of sodium oleate to 10.0 wt%, the contact angle was 104.99° (Fig. 6d).

3.3. Luminescence properties

The excitation and emission spectra of the obtained products are shown in Fig. 7. The excitation spectra contain a group of sharp lines in the longer wavelength region, which can be ascribed to the f–f transitions within the $4f^6$ configuration of Eu^{3+} ions. Upon excitation at 393 nm, the emission spectrum is composed of a group of lines peaking at around 579, 590, 613, 650 and 699 nm. They correspond to the $^5D_0$–^7F_J (J = 0, 1, 2, 3, 4)

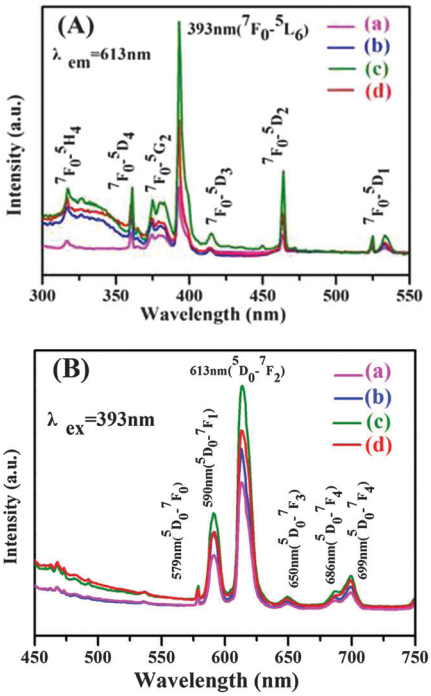

Fig. 7 The PL spectra of the products obtained with different amounts of sodium oleate: (a) 0.0% W_{CaCO_3}; (b) 2.0% W_{CaCO_3}; (c) 5.0% W_{CaCO_3}; and (d) 10.0% W_{CaCO_3}. (A) Excitation spectra and (B) emission spectra.

transition of the Eu^{3+} ions, respectively.[38] The strongest peak was located at 613 nm, which was the characteristic peak of Eu^{3+} ions.[39] However, the PL emission intensity of the obtained products increases with an increase in the amount of sodium oleate until the mass ratio of sodium oleate is 5.0%, and then decreases at a mass ratio of 10% sodium oleate. The enhancement is attributed to two functions of sodium oleate. One function is that sodium oleate can avoid OH ligands and/or crystal water molecules attached on the surface or in the host lattice of the $CaCO_3$ particle (as proved by IR and TGA); another function is that Na^+ ions supplied effective charge compensation. The reduction might be due to excess Na^+ ions and oleates, which are not beneficial to the luminescence. The trivalent activator like Eu^{3+} substitutes a divalent host cation, such as Ca^{2+}, and might form defects and destroy the lattice that in turn reduces the emission intensity. Therefore, charge compensation is needed to change the coordination conditions for Eu^{3+}, balance out the defects, reduce the crystal symmetry and break the parity-selection rules of the $^5D_0$–$^7F_2$ electric dipole transition to achieve the enhancement of Eu^{3+} emission.[40]

The mechanism in the charge compensation system is that two Ca^{2+} ions are replaced by one Eu^{3+} ion and one charge compensator ion.[41]

$$2Ca^{2+} \rightarrow Eu^{3+} + R^+ \ (R = Na^+, K^+)$$

When a trivalent metallic ion Eu^{3+} is incorporated into a host lattice and substitutes for a divalent metallic ion Ca^{2+}, the monovalent ion R^+ substitution would lead to charge balance as well as a reduction in Ca^{2+} vacancy concentration.[42] As a result,

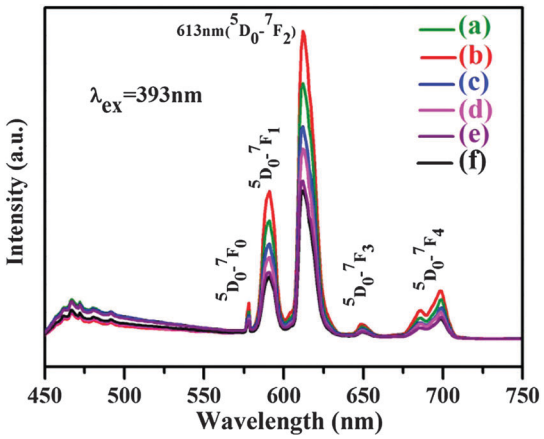

Fig. 8 PL spectra of $CaCO_3$:Eu^{3+} with different amounts of sodium oleate: (a) 5.0% W_{CaCO_3}; (b) 6.1% W_{CaCO_3} (the moles of Na^+ ions and Eu^{3+} ions are equal); (c) 7.0% W_{CaCO_3}; (d) 8.0% W_{CaCO_3}; (e) 9.0% W_{CaCO_3}; and (f) 10.0% W_{CaCO_3}.

the sub-lattice structure around the luminescent center is distorted, which adjusts its relative emission intensity and makes red emission enhancement possible.

Fig. 8 shows that the luminescence intensity of phosphors with the same moles of Na^+ ions and Eu^{3+} ions is stronger than that of other amounts of sodium oleate. The mechanism in the charge compensation system is that two Ca^{2+} ions are replaced by one Eu^{3+} ion and one charge compensator ion. The excess Na^+ ions and oleates are not beneficial to the luminescence. Therefore, the best ratio of Na^+ to Eu^{3+} is 1 : 1, in other words, the moles of Na^+ ions and Eu^{3+} ions doped should be equal.

In order to study the effect of charge compensation on the luminescence, we changed sodium oleate into potassium oleate and compared the luminescence of samples prepared with sodium oleate or potassium oleate. Fig. 9 shows the emission spectra of the samples prepared with different alkaline ions. At an excitation of 393 nm, the shapes of the emission spectra are very similar, indicating that the introduction of M^+ (M = Na, K) ions as charge compensation does not change the sub-lattice structure around the luminescent centre of Eu^{3+} ions.

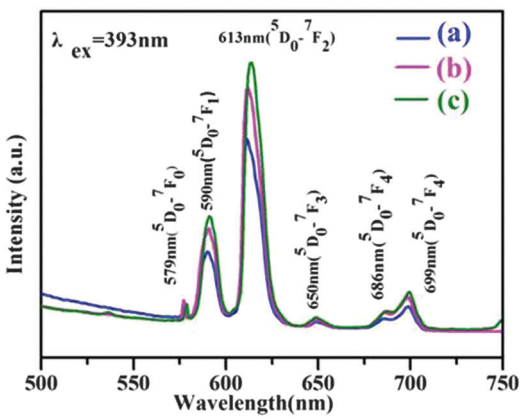

Fig. 9 Emission spectra of $CaCO_3$:Eu^{3+} prepared with (a) nothing, (b) 5.0 wt% potassium oleate, and (c) 5.0 wt% sodium oleate.

However, the luminescence intensity of phosphors with K^+ as charge compensation is weaker than that of phosphors co-doped by Na^+ and Eu^{3+}. It would be difficult for K^+ to enter the crystal lattice of $CaCO_3$:Eu^{3+} because the ionic radius of K^+ (138 pm) is 1.5 times greater than that of Ca^{2+} (99 pm) while the ionic radius of Na^+ (102 pm) is close to that of Ca^{2+}. Therefore, Na^+ ions can supply more effective charge compensation and make red emission stronger.

4. Conclusions

In summary, we demonstrate a simple, convenient and environmentally protectional, synthetic route to hydrophobic and enhanced red-emitting $CaCO_3$:Eu^{3+} phosphors. Without grinding, the prepared phosphors are present in powder form directly; without any further treatment such as sintering or calcination, the obtained powders show calcite crystals. The hydrophobic surface could not only endow good compatibility with plastics or other polymers but also reduce the OH ligands and/or crystal water molecules attached on the surface of $CaCO_3$ particles. On the other hand, Na^+ ions supplied effective charge compensation. All these result in enhanced red-emitting $CaCO_3$:Eu^{3+} phosphors. It is expected to provide a new idea for preparing efficient phosphors.

Acknowledgements

This work was financially supported by the National Natural Science Foundation of China (Grant no. 21171066 and 51272085) and the Opening Research Funds Projects of the State Key Laboratory of Inorganic Synthesis and Preparative (2013-27).

Note and references

1 H. Q. Liu, L. L. Wang, S. G. Chen and B. S. Zou, *J. Alloys Compd.*, 2008, **448**, 336–339.
2 Z. Y. Zhang, Y. H. Wang, J. C. Zhang and Y. Hao, *Mater. Res. Bull.*, 2008, **43**, 926–931.
3 C. Feldmann, T. Justel, C. R. Ronda and P. J. Schmidt, *Adv. Funct. Mater.*, 2003, **13**, 511–516.
4 I. Cacciotti, A. Bianco, G. Pezzotti and G. Gusmano, *Chem. Eng. J.*, 2011, **166**, 751–764.
5 N. Zhang, C. Guo and H. Jing, *RSC Adv.*, 2013, **3**, 7495–7502.
6 Y. H. Ko, S. H. Lee and J. S. Yu, *J. Nanosci. Nanotechnol.*, 2013, **13**, 3230–3235.
7 S. C. Prashantha, B. N. Lakshminarasappa and B. M. Nagabhushana, *J. Alloys Compd.*, 2011, **509**, 10185–10189.
8 J. R. M. Viana, M. J. Barboza, J. H. Rohling, A. C. Bento, M. L. Baesso and A. N. Medina, *Int. J. Thermophys.*, 2013, **34**, 1666–1672.
9 J. T. Lin and Q. M. Wang, *Chem. Eng. J.*, 2014, **250**, 190–197.
10 Y. Liu, Q. Ju and X. Chen, *Nanosci. Nanotechnol.*, 2012, **1**, 163–171.

11 K. Biswas, A. D. Sontakke, R. Sen and K. Annapurna, *J. Fluoresc.*, 2012, **22**, 745–752.
12 Q. Zhao, Y. H. Zheng, N. Guo, Y. C. Jia, H. Qiao, W. Z. Lv and H. P. You, *CrystEngComm*, 2012, **14**, 6659–6664.
13 G. W. Wang, H. F. Zou, H. G. Zhang, L. N. Gong, Z. Shi, X. C. Xu and Y. Sheng, *Mater. Lett.*, 2014, **128**, 256–258.
14 Q. B. Xiao, Y. S. Liu, L. Q. Liu, R. F. Li, W. Q. Luo and X. Y. Chen, *J. Phys. Chem. C*, 2010, **114**, 9314–9321.
15 M. Jiao, Y. Jia, W. Lü, W. Lv, Q. Zhao, B. Shao and H. You, *J. Mater. Chem. C*, 2014, **2**, 90–97.
16 H.-D. Nguyen, C. C. Lin, M.-H. Fang and R.-S. Liu, *J. Mater. Chem. C*, 2014, **2**, 10268–10272.
17 J. Q. Geng, D. Yang, J. H. Zhu, D. M. Chen and Z. Y. Jiang, *Mater. Res. Bull.*, 2009, **44**, 146–150.
18 J. Wang, Z. Peng, Y. Chen, W. Bao, L. Chang and G. Feng, *Chem. Eng. J.*, 2015, **263**, 9–19.
19 B. Souvereyns, K. Elen, C. De Dobbelaere, A. Kelchtermans, N. Peys, J. D'Haen, M. Mertens, S. Mullens, H. Van den Rul, V. Meynen, P. Cool, A. Hardy and M. K. Van Bael, *Chem. Eng. J.*, 2013, **223**, 135–144.
20 X. Jiang, Y. Pan, S. Huang, X. A. Chen, J. Wang and G. Liu, *J. Mater. Chem. C*, 2014, **2**, 2301–2306.
21 J. Gu, Y. W. Zhang and F. Tao, *Chem. Soc. Rev.*, 2012, **41**, 8050–8065.
22 M. Tukia, J. Holsa, M. Lastusaari and J. Niittykoski, *Opt. Mater.*, 2005, **27**, 1516–1522.
23 M. M. Wu, X. L. Li, G. P. Shen, J. Li, R. R. Xu and D. M. Proserpio, *J. Solid State Chem.*, 2000, **151**, 56–60.
24 M. Strek, P. Deren, A. Bednarkiewicz, M. Zawadzki and J. Wrzyszcz, *J. Alloys Compd.*, 2000, **300**, 456–458.
25 J. Nara and S. Adachi, *J. Appl. Phys.*, 2013, **113**, 033519.
26 J. Nara and S. Adachi, *ECS J. Solid State Sci. Technol.*, 2013, **2**, R135–R141.
27 M. Kang, J. Liu, R. Sun, G. F. Yin, X. M. Wang and W. Q. Yan, *Spectrosc. Spectral Anal.*, 2010, **30**, 225–229.
28 M. Kang, J. Liu, G. F. Yin and R. Sun, *Rare Met.*, 2009, **28**, 439–444.
29 B. Zhou, B. S. Liu, H. F. Zou, Y. H. Song, L. N. Gong, Q. S. Huo, X. C. Xu and Y. Sheng, *Colloids Surf., A*, 2014, **447**, 166–171.
30 Y. X. Pan, M. M. Wu and Q. Su, *Mater. Res. Bull.*, 2003, **38**, 1537–1544.
31 S. P. Bao, X. Y. Chen, Z. Li, B. J. Yang and Y. C. Wu, *CrystEngComm*, 2011, **13**, 2511–2520.
32 C. M. Chan, J. S. Wu, J. X. Li and Y. K. Cheung, *Polymer*, 2002, **43**, 2981–2992.
33 X. F. Zeng, W. Y. Wang, G. Q. Wang and J. F. Chen, *J. Mater. Sci.*, 2008, **43**, 3505–3509.
34 Y. X. Chen, X. B. Ji, G. Q. Zhao and X. B. Wang, *Powder Technol.*, 2010, **200**, 144–148.
35 L. Guo and B. Yan, *J. Photochem. Photobiol., A*, 2011, **224**, 141–146.
36 C. Y. Wang, P. Xiao, J. Z. Zhao, X. Zhao, Y. H. Liu and Z. C. Wang, *Powder Technol.*, 2006, **170**, 31–35.
37 Y. Sheng, B. Zhou, C. Y. Wang, X. Zhao, Y. H. Deng and Z. C. Wang, *Appl. Surf. Sci.*, 2006, **253**, 1983–1987.
38 Z. Lu, L. Chen, Y. Tang and Y. Li, *J. Alloys Compd.*, 2005, **387**, L1–L4.
39 Z. W. Tang, L. Q. Zhou, L. Yang and F. Wang, *J. Lumin.*, 2010, **130**, 45–51.
40 A. Xie, X. M. Yuan, F. X. Wang, Y. Shi and Z. F. Mu, *J. Phys. D: Appl. Phys.*, 2010, **43**, 055101.
41 E. L. Cates, A. P. Wilkinson and J. H. Kim, *J. Phys. Chem. C*, 2012, **116**, 12772–12778.
42 X. Y. Yang, J. Liu, H. Yang, X. B. Yu, Y. Z. Guo, Y. Q. Zhou and J. Y. Liu, *J. Mater. Chem.*, 2009, **19**, 3771–3774.